SAND 2000-8515C

# MECHANISMS OF SILICA REFRACTORY CORROSION IN GLASS-MELTING FURNACES: EQUILIBRIUM PREDICTIONS

Karl E. Spear, Materials Science and Engineering, Pennsylvania State University, University Park, PA 16802
Mark D. Allendorf, Sandia National Laboratories, Livermore, CA 94551-0969

Corrosion of refractory silica brick used to line the roof or "crown" of many-glass-melting furnaces is a serious problem in furnaces using oxygen-fuel rather than air-fuel. In this work, we report equilibrium calculations for the $Na_2O$-$SiO_2$ system that predict the formation of a variable-composition liquid-solution phase as a function of key furnace variables. Since thermodynamic data for the relevant liquid phases are unavailable in standard compilations, new data generated using the associate species model are included in the calculations. The calculations indicate that gas-phase NaOH concentrations less than ~15 ppm will not react with the silica refractory under either air-fired or oxy-fired conditions, since this is the smallest equilibrium NaOH partial pressure in a system containing crystalline $SiO_2$ (either cristobalite or tridymite) in equilibrium with a variable-composition sodium-silicate liquid phase at refractory temperatures in the range 1400 – 1700 °C. The high water content (~65%) of oxygen-fired furnaces results in measured NaOH(g) concentrations as high as 300 ppm, which greatly exceeds the 1600°C maximum of 68 ppm NaOH(g) for oxy-fired equilibrium with a liquid-SiO2(crystalline) system. This indicates that there is a thermodynamic driving force for NaOH(g) to react with silica refractories in oxy-fired furnaces. The results of the calculations are used to define a "critical temperature," above which corrosion is not expected to occur for a given NaOH(g) partial pressure.



## INTRODUCTION

Refractory brick composed primarily of silica is commonly used to line the interiors of glass-melting furnaces. In air-fired furnaces, the furnace roof or "crown" typically lasts on the order of ten years. Recently, however, the replacement of air with pure oxygen in the combustion gases in many melting furnaces has lead to substantially higher silica corrosion rates.[1] In some cases, crown lifetimes decreased by as much as a factor of two. The high cost of rebuilding these furnaces is driving organized efforts to determine the factors controlling corrosion, so that either furnace conditions can be adjusted to reduce corrosion to acceptable rates, or alternative refractory materials can be identified that are more inert. The former solution is preferable, since silica brick is attractive because of its low density (which simplifies furnace construction), low thermal conductivity, and low cost.

A major component of many glasses is sodium, which in the presence of combustion-generated water vapor is converted to gas-phase sodium hydroxide. It is known that the concentration of NaOH(g) in oxy-fuel furnaces is as much three to four times higher than in air-fired furnaces,[2] most likely due to higher water-vapor concentrations in the furnace atmosphere. Although this is undoubtedly linked to the higher corrosion rates, the situation is more complex than this. Both temperature[3] and gas velocity[4] may play important roles. Thus, a full understanding of the corrosion process will undoubtedly have to account for all of these parameters. In spite of this, chemical reactions remain at the heart of the process. Since the temperatures of the silica refractory are typically quite high, ranging from more than 1600°C at the surface exposed to the furnace to above 1100°C on the exterior side of an insulated crown, equilibrium represents a reasonable approximation of the chemical behavior of the corrosion processes. Thus, thermodynamic calculations (i.e., predictions of chemical compositions based on minimization of the Gibbs free energy) can play a useful role by identifying

## DISCLAIMER

energetically stable species and by predicting the actual extent of corrosion and corrosion products.

Previous investigations of the equilibrium thermodynamics of the $Na_2O$-$SiO_2$-[3,5] system revealed several trends in the conversion of silica to sodium silicates. However, these calculations did not consider the formation of liquid phases, since thermodynamic data for only crystalline phases was available at the time. As a result, there may be systematic errors in the conclusions deduced from these previous results. Furthermore, no equilibrium constant is given for what is claimed to be the primary corrosion reaction [$2NaOH(g) + 2SiO_2(c) \leftrightarrow Na_2O.2SiO_2(c) + H_2O(g)$]; thus, these results are of limited value for the development of quantitative kinetic models of the corrosion process.

The accuracy of a thermodynamic calculation depends, of course, on the quality and completeness of the data employed. In the case of alkali corrosion of silica, the observed products are often low-melting glasses containing various amounts of $Na_2O$ and $SiO_2$. Although the thermodynamics of the sodium oxide/silica system have been extensively studied due to its importance in a variety of fields,[6,7] this system is quite complex and descriptions based on ideal ionic solutions have uniformly failed. Alternative methods are needed to determine accurate thermodynamic functions for the low-melting corrosion products. Several such methods have been applied with varying degrees of success, including the quasi-chemical model of Pelton and coworkers[6] and a model based on the associated-solution theory.[7]

In this work, we use an associate species model[8] for describing the thermodynamic functions for the liquid phases in the $Na_2O$-$SiO_2$ system. We then include these data in calculations of the equilibrium between silica and typical air- and oxy-fuel-fired glass-melting atmospheres. These are the first calculations to assess the impact of the formation of sodium-silicate glasses on the corrosion of silica. The results reported here include: the temperature dependence of the gas-phase sodium-containing species concentrations; the composition of corrosion products and their temperature dependence; and predicted temperature and NaOH concentration regimes in which corrosion of silica is expected to occur. Finally, we use these results to suggest mechanisms that may be active in the corrosion process.

## CORROSION REACTIONS AND EQUILIBRIUM MODELING

Calculations show that NaOH(g) is the most abundant gaseous species containing sodium at equilibrium between combustion atmospheres and sodium-containing glass melts. Therefore, we have assumed that NaOH(g) is the key sodium-containing species participating in the corrosion of silica. Its formation can be described by the following chemical reaction:

$$Na_2O(\text{in glass melt}) + H_2O(\text{g, combustion gas}) \leftrightarrow 2NaOH(g) \quad (1)$$

At the surface of the refractory, a second reaction occurs to form a silica-rich, liquid solution in which $Na_2O$ is dissolved. This liquid phase is in local equilibrium with the $SiO_2$(cristobalite) refractory:

$$2NaOH(\text{gas}) \leftrightarrow Na_2O(\text{dissolved in liquid } SiO_2) + H_2O(\text{g, combustion gas}) \quad (2)$$

To model these reactions at equilibrium, one needs to know the partial pressure of $H_2O(g)$ ($p_{H2O}$) and the activity of $Na_2O$ ($a_{Na2O}$) as a function of temperature and composition, as well as the equilibrium constant $K_{eq}$ for Reactions 1 and 2 (which is also a function of temperature).

The partial pressure of $H_2O$ in the combustion gas at the furnace-gas temperature can be predicted from an equilibrium calculation using a knowledge of the input combustion-gas mixture. However, heat losses, which are difficult to predict, play a critical role in determining the actual temperature. The results of such calculations show, however, that $p_{H2O}$ varies very little over the temperature range of interest (1400 – 1700°C) since the combustion reaction to produce water and carbon dioxide is fairly complete under these conditions. It is thus realistic to use a fixed value of $p_{H2O}$ at all temperatures of interest. Input parameters used in an equilibrium calculation to determine this value are given in Table I. The input conditions were chosen so that the condensed equilibria were always a mixture of liquid and crystalline silica. The liquid was a solution of $Na_2O$ in liquid silica.

**Table I.** Typical input conditions for equilibrium calculations.
P(total) = 1 bar, T = 1400 to 1700°C

| | $n(CH_4)^a$ | $n(O_2)^a$ | $n(N_2)^a$ | $n(Na_2O)^a$ | $a(SiO_2)^b$ |
|---|---|---|---|---|---|
| Calculation of $p_{H2O}$ | | | | | |
| Air-fired | 1.00 | 2.05 | 8.2 | -- | -- |
| Oxy-fired | 1.00 | 2.05 | -- | -- | -- |
| Corrosion predictions | | | | | |
| Air-fired | 1.00 | 2.05 | 8.2 | 0.1 | 1.0 |
| Oxygen-fired | 1.00 | 2.05 | -- | 0.1 | 1.0 |

[a] Moles. [b] Activity of $SiO_2$(crystalline) was fixed at unity.

To determine $a_{Na2O}$ in the liquid and thus be able to predict the corrosion of crystalline silica, reliable high-temperature thermodynamic and phase-equilibria data are required for all critical species and phases in the $Na_2O$–$SiO_2$–$H_2O$ system. These data are available for most of the combustion gases involved, although the range of reported values for the heat of formation for NaOH is somewhat larger than expected (see below). Tabulated thermodynamic data for liquid-phase corrosion products are lacking, so these values were determined along with an assessment and optimization of the values for crystalline phases in the $Na_2O$-$SiO_2$ binary system. The computer program ChemSage™ [9] is our primary tool for developing an assessed, internally consistent thermodynamic database for the $Na_2O$-$SiO_2$ system, and for performing subsequent calculations of the high-temperature corrosion reactions between NaOH(g) and $SiO_2$(s). The following paragraphs describe our analysis of the available data for this system and our choices for the values used in the equilibrium calculations described later in the paper.

The required thermodynamic data for most gas-phase species were obtained from the assessed SGTE database.[10] However, the $\Delta H^\circ_{f,298}$ value for NaOH(g) in this database (-185.649 kJ/ mol ) is quite different from that found in the *JANAF Thermochemical Tables* (-197.757 kJ/mol).[11] The corresponding values of the entropy ($S^\circ_{298}$) from these two sources are quite similar, however, being 228.589 and 228.443 J/mol-K, respectively. The $\Delta H^\circ_{f,298}$ and $S^\circ_{298}$ values for the solid (NaOH(s)) from the two sources are essentially the same. Thus, the 12 kJ/mol difference in the $\Delta H^\circ_{f,298}$ values for the vapor species appears to be the only major uncertainty in the sodium hydroxide data used in our calculations. Communications with the Russian group responsible for the IVANTHERMO database (Gorokhov et al.)[12] revealed that their experimental mass-spectrometric measurements of NaOH vapor pressures yield a $\Delta H^\circ_{f,298}$ of –189.7 ± 4 kJ/mol. The IVANTHERMO Database[13] has assessed this value to be –191.0 ± 8 kJ/mol. Both of these values lie between the SGTE and JANAF values. In the calculations described here, we chose to use the *JANAF* value for $\Delta H^\circ_{f,298}$(NaOH,g). However, Figure 6 shows the effect of difference in the SGTE and JANAF values in predicting the critical boundary lines that separate corrosive from non-corrosive conditions for air-fired and oxygen-fired furnaces (see discussion below). This provides a measure of the uncertainty

in quantitative numbers produced by our calculations. However, the general explanations of the observed corrosion behavior are not changed.

The thermodynamic data for the binary $Na_2O$-$SiO_2$ system were assessed and optimized by performing a "thermodynamic fitting" of the binary equilibrium phase diagram for this system. This procedure provides a means of testing and generating a set of self-consistent thermodynamic information for the system, including thermodynamic data for the oxide liquid phase.[8] The resulting calculated phase diagram is shown in Figure 1 for this system and is in agreement with the assessed diagram given by Eriksson et al.,[6] except for omitting the questionable $Na_6SiO_7$ and $Na_6Si_8O_{19}$ phases. The important portion of the diagram for this study of silica refractory corrosion is the high temperature $SiO_2$-rich two-phase region of $SiO_2$-liquid. The liquid in this two-phase mixture is a product of reactions between NaOH(g) and $SiO_2$(s). The thermodynamic model used for the liquid phase is discussed below.

Accurate values of the thermodynamic data for liquid-oxide solutions is of critical importance to our thermodynamic description of the $Na_2O$-containing liquid corrosion product. To obtain these values, we modeled the liquid using an associate species model described previously.[8] This model uses intermediate "chemical species" with their corresponding thermodynamic data to represent the negative free-energy terms caused by nonideal mixing of the end-member components in a system. For example, in the $Na_2O$-$SiO_2$ binary system, the liquid is composed of "liquid species" $Na_2O$, $(2/5)Na_4SiO_4$, $(2/3)Na_2SiO_3$, $(1/2)Na_2Si_2O_5$, and $Si_2O_4$. To provide equal weighting to each liquid associate species, each species has a total of two non-oxygen atoms in its formula. While these liquid species may not exist as chemical entities that can be isolated and characterized, they can accurately represent the negative interaction energies that occur between $Na_2O$ and $SiO_2$ in this liquid oxide solution. Positive interactions (repulsion terms ultimately leading to phase separation in solutions) cannot be modeled using the associate species model; instead, we used Redlich-Kister constants between the associate species $(1/2)Na_2Si_2O_5$ and $Si_2O_4$ to accurately model the composition region in which a metastable immiscibility gap has been reported for glass phases in this system (see the phase diagram in Figure 1 for $X(SiO_2) > 0.8$ and $T < 850^{\circ}C$).

The major species included in the various calculations are given in Table II, which also includes the source for the thermodynamic data in each case. All calculations were performed for a total pressure of 1 bar. In modeling the corrosion of silica refractory, a large excess of silica ($SiO_2$ in its most stable form at each temperature) was used to represent the refractory, so that in all cases the calculations predict the existence of some crystalline silica at equilibrium.

**Table II.** Major species used in calculations and sources of thermodynamic data.

| **Gas-phase** [a] | | | | |
|---|---|---|---|---|
| $N_2$ | $H_2O$ | $CH_4$ | $O_2$ | NO |
| $H_2$ | OH | $CO_2$ | $NO_2$ | $N_2O$ |
| H | CO | HCN | $NH_3$ | |
| $SiO_2$ | SiO | Na | NaOH[b] | |
| **Liquid phase**[c] | | | | |
| $Na_2O$(l) | $(2/5)Na_4SiO_4$ | $(2/3)Na_2SiO_3$ | $(1/2)Na_2Si_2O_5$ | $Si_2O_4$ |
| **Solid phases** [c] | | | | |
| $SiO_2$ (cristobalite) | $SiO_2$ (tridymite) | $SiO_2$ (quartz) | $Na_2Si_2O_5$ | $Na_2SiO_3$ |
| $Na_4SiO_4$ | $Na_2O$ | | | |

[a] A total of 75 species were initially used in these calculations. The major source of these data was *SGTE* (Ref. 10) except as noted. [b] *JANAF* (Ref. 11). [c] A total of 15 fixed composition phases were initially used in these calculations. The source of the listed liquid and solid phase data was assessments described in Ref. 8, and the current work.

## RESULTS

### Prediction of the $Na_2O$-$SiO_2$ Phase Diagram

To model the corrosion of silica refractories, we first determined thermodynamic data for sodium-containing silica-rich liquid phase (the expected product of silica corrosion by NaOH(g)) using the associate species model. The results of these calculations are shown in Figure 1 in the form of the phase diagram for the $Na_2O$-$SiO_2$ system. This diagram is in good agreement with the experimental and assessed phase diagram for the well-established crystalline phases of $Na_4SiO_4$, $Na_2SiO_3$, and $Na_2Si_2O_5$.[6] The important portion of the diagram for this corrosion study is the two-phase region in which crystalline silica (either cristobalite or tridymite) is in equilibrium with a liquid of composition $(SiO_2)_x(Na_2O)_{1-x}$. Figure 2 shows an expanded version of this important $SiO_2$-rich portion of the diagram. The thermodynamic data for the $SiO_2$-rich liquid predict the observed metastable liquid phase separation (immiscibility) that occurs at temperatures below about 850°C in the $X(SiO_2) > 0.8$ portion of the diagram. Phase transition temperatures for $SiO_2$(s) are also in good agreement with reported values.

### Equilibrium Predictions of Silica Corrosion

Figure 1 reveals a key result of these calculations: in the glass melting furnace atmosphere and temperatures, crystalline silica in the refractory can react with NaOH(g) to produce an equilibrium product of a silica-rich liquid containing dissolved $Na_2O$. Although crystalline sodium silicates such as $Na_2Si_2O_5$ and $Na_2SiO_3$ are included in the calculations (Table II), none are predicted to form. The $Na_2O$ mole fraction of the liquid corrosion product varies between zero at the 1723°C melting point of cristobalite to more than 0.24 at 815°C. We note, however, that the refractory temperature in actual glass-melting furnaces is routinely much higher than 815 °C for an insulated crown, which is typical of most furnaces in operation today.[14] (Temperatures as low as 370 °C can occur when the cold side of the crown is uninsulated. However, equilibrium calculations for representing experimental behavior will almost certainly be invalid at such low temperatures, since the approach to equilibrium is so slow.) Consequently, we also show an expanded view of the phase diagram in Figure 2 for the 1400 – 1700 °C temperature range of interest for corrosion on the hot face of the refractory.

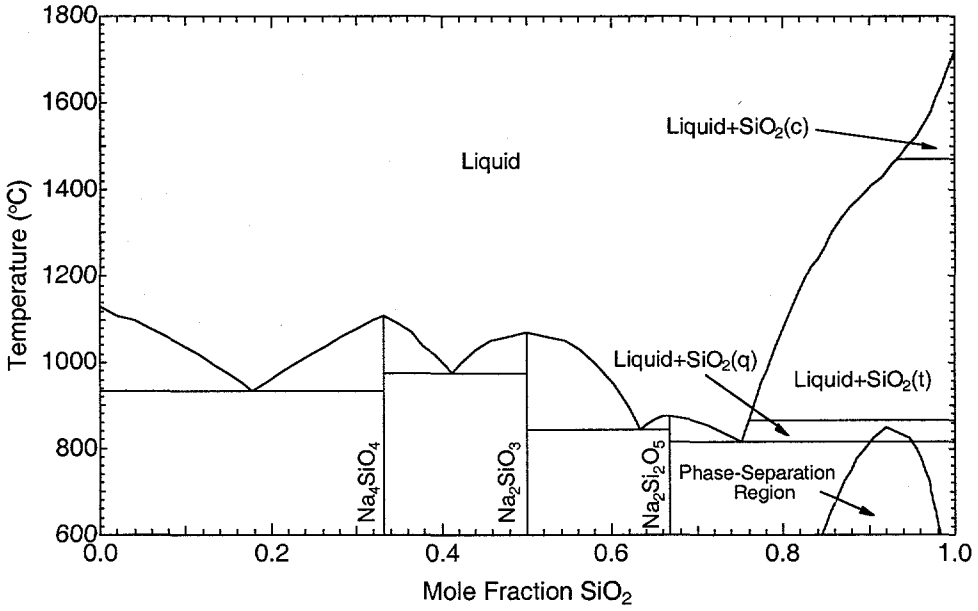


**Figure 1.** Calculated phase diagram for the $SiO_2$-$Na_2O$ system.

Selected results of fixed-temperature equilibrium calculations for two typical combustion mixtures (see Table I) are shown in Figures 3 – 5. The gas-phase concentrations shown correspond to the situation when crystalline silica is in equilibrium with a liquid phase containing $SiO_2$ and varying amounts of $Na_2O$. For purposes of this discussion, we assume that some corrosion of the refractory will occur if the equilibrium calculation predicts the formation of a liquid sodium-silicate solution, as described by Reaction 2.

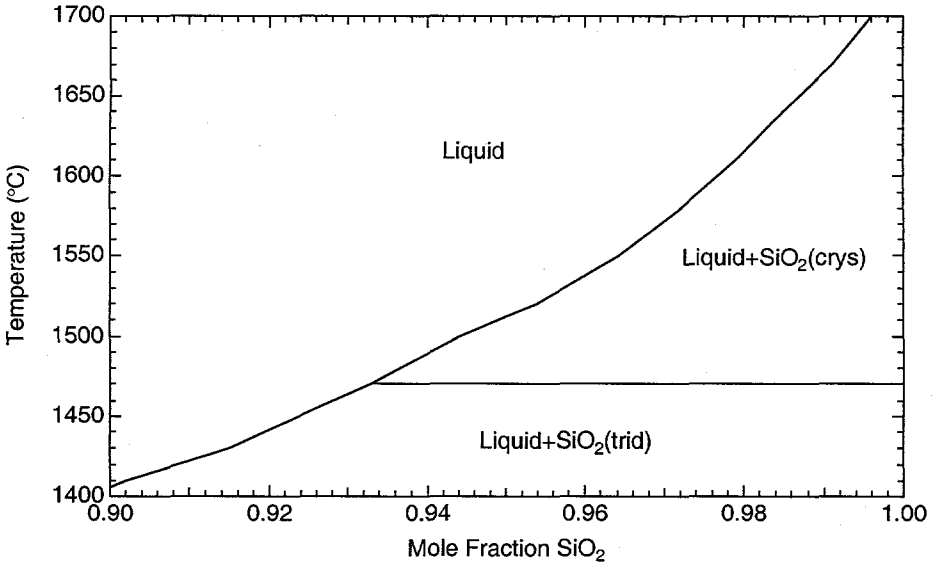


**Figure 2.** Expanded view of the silica-rich region of the $Na_2O$-$SiO_2$ phase diagram shown in Figure 1.

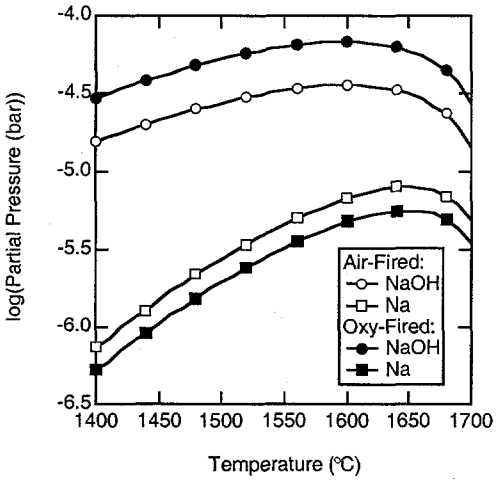


**Figure 3.** Partial pressures of NaOH and Na as a function of temperature and input-gas composition.

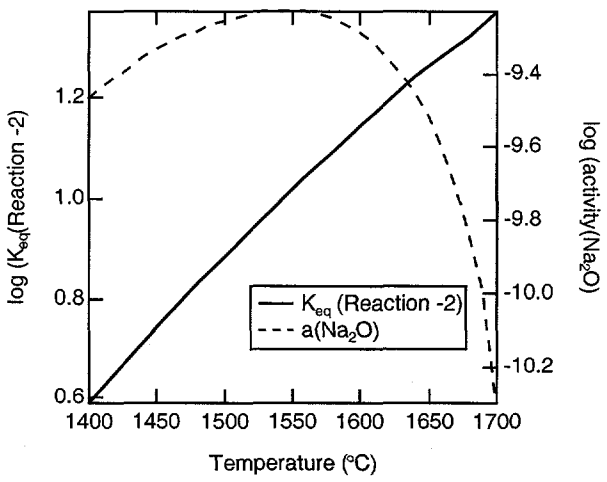


**Figure 4.** Temperature dependence of the equilibrium constant for Reaction (-2), with the $Na_2O$ activity in the liquid phase.

Figure 3 yields two important results. First, NaOH(g) is the dominant sodium-containing species in the gas, significantly exceeding the sodium-atom concentration at all temperatures. Equilibrium concentrations of NaOH(g) are always about a factor of two higher in oxy-fired furnace atmospheres than those predicted for air-fired furnace atmospheres. For example, the maximum NaOH(g) equilibrium partial pressure under air-fired conditions is about 36 ppm, while under oxy-fired conditions, it is about 68 ppm (both maxima occur at ~ 1600°C). This is due to the higher water-vapor concentration under oxy-fired (e.g. mole fraction $H_2O$ = 0.654 at 1600°C) vs. air-fired (e.g. mole fraction $H_2O$ = 0.177 at 1600°C) conditions, which shifts the equilibrium of Reaction 2 to the left. It is important to note that these NaOH(g) concentrations are significantly smaller than those determined by the Faber and Verheijn in their equilibrium calculations,[5] but they considered only the formation of crystalline sodium silicates as corrosion products. In their report, these authors determined the equilibrium concentration of NaOH(g) in equilibrium with $Na_2Si_2O_5$-$SiO_2$ would be 60 ppm under air-fired conditions at 1269°C, and would be 220 ppm under oxy-fired conditions at 1408°C. In contrast, our calculations, which result in a liquid corrosion product in equilibrium with $SiO_2$, yield 6.3 ppm and 31 ppm, respectively, at these temperatures and conditions. Thus, our results suggest that the NaOH(g) concentration at which corrosion will occur at a given temperature is significantly lower than was previously predicted.

A second noteworthy result obtained from Figure 3 is that the equilibrium concentration of NaOH under both sets of conditions peaks at a temperature of ~ 1600°C. This results from a combination of two competing effects. The decreasing concentration (activity) of $Na_2O$(l) in the liquid corrosion product with increasing temperature (Figure 4, dashed line) ultimately causes the NaOH(g) concentration to decrease at higher temperatures. Counteracting this effect, however, and leading to the maximum in the NaOH(g) concentration, is the increase with temperature in the equilibrium constant for the reaction $Na_2O(l) + H_2O(g) \leftrightarrow 2NaOH(g)$ (Figure 4). This maximum has some interesting consequences with regard to the regions in which corrosion is predicted to occur; this is discussed in detail below.

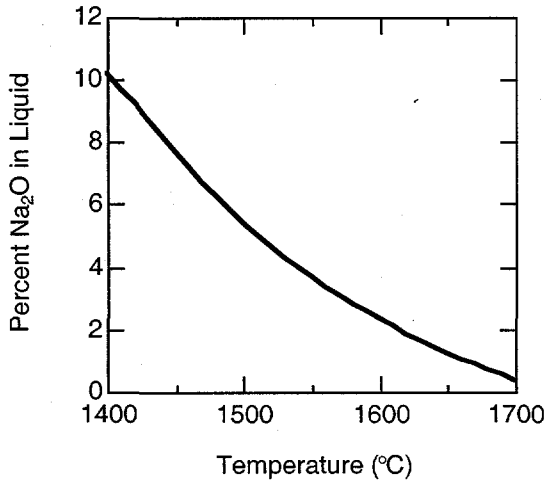


**Figure 5.** Percent $Na_2O$ in liquid corrosion product as a function of temperature.

Figure 5 shows that the mole fraction of $Na_2O$ ($X_{Na2O}$) dissolved in the liquid silica corrosion product decreases with increasing temperature as long as equilibrium exists between the liquid and $SiO_2$(crystalline). At the lowest temperature shown (1400°C), the

mole fraction is ~10%. As the temperature increases, this value decreases, ultimately becoming zero at 1723°C, the melting point of pure cristobalite. This has important consequences for the development of corrosion mechanisms, since increasing $Na_2O$ concentrations are known to reduce the viscosity of sodium silicate melts.[14,15]

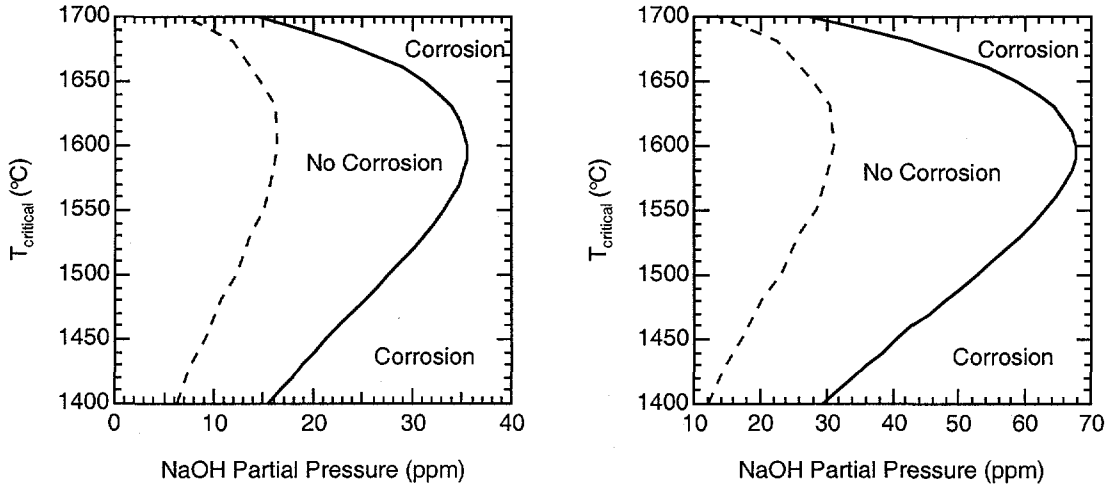


**Figure 6.** Zones of corrosion as a function of gas-phase partial pressure of NaOH, as defined by $T_{critical}$ (see text). Left: air-fired conditions; Right: oxy-fired conditions. Note the horizontal scales on the two plots are not the same. Data from the *JANAF Tables* were used to obtain the solid curves. The dashed lines indicate predictions obtained from the SGTE database (see text); the labels "Corrosion" and "No Corrosion" apply only to the solid curves.

The curves in Figure 6 show that, for a given $p_{NaOH}$, there are temperature regions in which corrosion will occur and where it will not occur. In general, corrosion occurs (i.e., a liquid sodium silicate phase forms) in the region of conditions to the right of each curve. For example, if the $p_{NaOH}$ in the combustion atmosphere is higher than that in equilibrium with crystalline silica and the liquid sodium silicate phase (the boundary line in Figure 6), then corrosion can occur. The lower portion of the curves in Figure 6 thus defines a "critical temperature," above which corrosion does not occur for a given $p_{NaOH}$ in the combustion atmosphere. This concept was introduced previously by Faber and Verheijn,[5] but not published in the open literature. Above the lower branch of the solid curve, corrosion will not occur since $p_{NaOH}$ is below the equilibrium value. These results are again consistent with the observations in actual furnaces, which show that insulating the cold side of the crown refractory, and thus increasing the temperature of the hot face, slows the rate of corrosion.[16]

Interestingly, the results in Figure 6 suggest that, if sufficiently high temperatures are reached (i.e., above the upper branch of the curves), corrosion should resume, since the NaOH concentration will again exceed the equilibrium value. This is a direct consequence of the fact that there is a maximum in the $p_{NaOH}$ vs. temperature curve (Figure 3). Practically speaking, the amount of corrosion might be very small at these temperatures since the calculations reveal that the amount of $Na_2O$ in the liquid corrosion product decreases as temperature increases (Figures 2 and 5), leading to more viscous liquids that could pose a transport limitation to the reaction. At concentrations above ~36 ppm (air-

fired) or ~68 ppm (oxy-fired), corrosion can occur at all temperatures since $p_{NaOH}$ is always above the liquid-$SiO_2$(crystalline) equilibrium value.

Finally, the two curves show that the region in which corrosion occurs shifts to higher $p_{NaOH}$ (at a given temperature) as one shifts from an air-fired to an oxy-fired furnace (i.e., as the concentration of water vapor in the furnace atmosphere increases). However, this result can be misleading if one does not take into account the fact that air-fired combustion atmospheres contain lower concentrations of NaOH(g) than oxy-fired atmospheres because of the higher water concentrations in the oxy-fired furnaces.

These results suggest a mechanism that could be responsible for the phenomenon known as "ratholing," in which large voids form in the interior of the crown refractories. These voids are typically connected to the hot face of the refractory via a narrow channel. The initial formation of the channel may be caused by relatively slow corrosion, perhaps along a joint or originating in at a defect of some kind. After reaching relatively cooler regions in the interior of the refractory, however, corrosion may accelerate since there is a stronger thermodynamic driving force at lower temperatures. This driving force results from two factors: first, lower temperatures lead to lower equilibrium $p_{NaOH}$ (Figure 3). Second, lower temperatures also favor liquid corrosion products containing higher concentrations of sodium (Figure 5). As a result, if the $p_{NaOH}$ in the channel at some point in the interior of the refractory exceeds the equilibrium value, the excess NaOH will react with the refractory to form more of the liquid-phase corrosion product, which will then reduce $p_{NaOH}$ and increase the fraction of $Na_2O$ in the liquid phase. As mentioned previously, increasing the concentration of sodium in the liquid phase reduces its viscosity.[14,15] Hence, liquid products formed at cooler temperatures may be more prone to flow back out the original entrance channel than more viscous ones formed at higher temperatures. This constant removal of reaction product could maintain a condition in which fresh refractory is continuously exposed to gas-phase NaOH, leading to continued corrosion and thus, the opening of an interior void. This mechanism, if true, confirms strategies currently used by the industry to avoid ratholing, namely, 1) insulating the back (cool) side of the refractory to minimize the temperature gradient and 2) taking great care to avoid openings in joints through which corrosive gases can travel to cooler portions of the refractory.

## SUMMARY AND CONCLUSIONS

The results of equilibrium calculations for the $Na_2O$-$SiO_2$ system are reported and indicate that the principal product of the corrosion of $SiO_2$ refractories by gas-phase NaOH is a molten glass containing variable amounts of sodium. The amount of sodium in this product increases with decreasing temperature. Since increasing sodium correlates with decreasing viscosity, the results suggest that higher refractory temperatures could inhibit corrosion by promoting the formation of products that are less prone to flow away from the surface. This result confirms anecdotal evidence available from the glass-manufacturing industry. The calculations also indicate that a critical temperature may exists at a given $p_{NaOH}$ above which corrosion is not thermodynamically favored to occur, since the equilibrium NaOH vapor pressure is higher than that existing in the furnace atmosphere. Together, these results suggest a mechanism whereby temperature gradients across the refractory crown of a glass-melting furnace could lead to formation of interior voids in the refractory (also known as "ratholing"). In future reports, we will discuss the use of these results in the development of models that account for both chemical reactions and transport phenomena in the corrosion of silica refractory. We will also extend the calculations to the $K_2O$-$SiO_2$ system and will describe these results in an upcoming report.[15]

ACKNOWLEDGMENTS

We would like to thank Drs. Larry Baxter (Sandia), Robert Nilson (Sandia), and George Pecoraro (PPG Industries, Inc.) for technical assistance in the writing of this article. For their financial support, we are grateful to: the U.S. Dept. of Energy (DOE) Office of Industrial Technologies Glass Industry of the Future Team; American Air Liquide, BOC Gases, PPG Industries Inc., Praxair Inc., Techneglas, and Visteon Automotive Systems; and the DOE Environmental Management Science Program funded by the Office of Environmental Management's Office of Science and Technology, and administered jointly with the Office of Energy Research under contract DE-AC05-96OR22464 with Lockheed Martin Energy Research Corporation.

REFERENCES

1. Pecoraro, G. A.; Marra, J. C.; Wenzel, J. T., (ed.), *Corrosion of Materials by Molten Glass*, American Ceramic Society, Westerville, 1996.
2. Boillet, J.; Paskocimas, C. A.; Leite, E. R.; Longo, E.; Varela, J. A.; Kobayashi, W. T.; Snyder, W. J. in G. A. Pecoraro, J. C. Marra and J. T. Wenzel (ed.), *Corrosion of Materials by Molten Glass, Ceramic Trans. Vol 78*, American Ceramic Society, Westerville, 1996, p. 217.
3. Slade, S. J. in G. A. Pecoraro, J. C. Marra and J. T. Wenzel (ed.), *Corrosion of Materials by Molten Glass*, American Ceramic Society, Westerville, 1996, p. 195.
4. Wu, K. T.; Kobayashi, H. in G. A. Pecoraro, J. C. Marra and J. T. Wenzel (ed.), *Corrosion of Materials by Molten Glass*, American Ceramic Society, Westerville, 1996, p. 205.
5. Faber, A. J.; Verheijen, I. O. S. "Report NCNG-project: Reduction of Refractory Corrosion-Phase 1," TNO Institute of Applied Physics HAM-RPT-96396, 1996.
6. Wu, P.; Eriksson, G.; Pelton, A. D., *J. Am. Ceram. Soc.*, **76** (1993), 2059.
7. Zaitsev, A. I.; Shelkova, N. E.; Lyakishev, N. P.; Mogutnov, B. M., *Phy. Chem. Chem. Phys.*, **1** (1999), 1899.
8. Spear, K. E.; Besmann, T. M.; Beahm, E. C., *MRS Bull.*, **24** (1999), 37.
9. "ChemSage™ 4.1," GTT Technologies, Herzogonrath, Germany 1998.
10. "SGTE Pure Substance Database, 1996 Version," produced by the Scientific Group Thermodata Europe and obtained through GTT Technologies (see Ref. 9).
11. Chase Jr., M. J., *J. Phys. Chem. Ref. Data, Monograph 9*, (1998), 1.
12. Gorokhov, L. N.; Emelyanov, A. M., *Russ. J. Phys. Chem.*, **70** (1996), 1003.
13. Gurvich, L. V.; Bergman, G. A.; Gorokhov, L. N., *J. Phys. Chem. Ref. Data*, **25** (1996), 1211.
14. Bockris, J. O. M.; MacKenzie, J. D.; Kitchener, J. A., *Trans. Faraday Soc. (London)*, **51** (1955), 1734.
15. Bansal, N. P.; Doremus, R. H. *Handbook of Glass Properties*, Academic, Orlando, 1986.
16. LeBlanc, J., *Ceram. Ind.*, **146** (1996), 27.